



OPEN ACCESS

EDITED BY

Menghao Huang,
Indiana University Bloomington,
United States

REVIEWED BY

Jimin Park,
Indiana University, Purdue University
Indianapolis, United States
Myeongjin Yi,
National Institute of Environmental
Health Sciences (NIH), United States

*CORRESPONDENCE

Ren-Ai Xu,
✉ xra@wmu.edu.cn

[†]These authors have contributed equally
to this work

RECEIVED 11 September 2023

ACCEPTED 08 November 2023

PUBLISHED 28 November 2023

CITATION

Nie J, Xia H, Liu Y-N, Yu Y and Xu R-A
(2023), Inhibitory effect of napabucasin
on arbidol metabolism and its
mechanism research.
Front. Pharmacol. 14:1292354.
doi: 10.3389/fphar.2023.1292354

COPYRIGHT

© 2023 Nie, Xia, Liu, Yu and Xu. This is an
open-access article distributed under the
terms of the [Creative Commons
Attribution License \(CC BY\)](https://creativecommons.org/licenses/by/4.0/). The use,
distribution or reproduction in other
forums is permitted, provided the original
author(s) and the copyright owner(s) are
credited and that the original publication
in this journal is cited, in accordance with
accepted academic practice. No use,
distribution or reproduction is permitted
which does not comply with these terms.

Inhibitory effect of napabucasin on arbidol metabolism and its mechanism research

Jingjing Nie^{1,2†}, Hailun Xia^{3†}, Ya-Nan Liu², Yige Yu² and Ren-Ai Xu^{2*}

¹Department of Pharmacy, The Third Affiliated Hospital of Wenzhou Medical University, Wenzhou, Zhejiang, China, ²Department of Pharmacy, The First Affiliated Hospital of Wenzhou Medical University, Wenzhou, Zhejiang, China, ³Key Laboratory of Diagnosis and Treatment of Severe Hepato-Pancreatic Diseases of Zhejiang Province, The First Affiliated Hospital of Wenzhou Medical University, Wenzhou, Zhejiang, China

As a broad-spectrum antiviral, and especially as a popular drug for treating coronavirus disease 2019 (COVID-19) today, arbidol often involves drug–drug interactions (DDI) when treating critical patients. This study established a rapid and effective ultra-performance liquid chromatography–tandem mass spectrometry (UPLC–MS/MS) method to detect arbidol and its metabolite arbidol sulfoxide (M6-1) levels *in vivo* and *in vitro*. In this study, a 200 μ L incubation system was used to study the inhibitory effect of the antitumor drug napabucasin on arbidol *in vitro*, with IC₅₀ values of 2.25, 3.91, and 67.79 μ M in rat liver microsomes (RLMs), human liver microsomes (HLMs), and CYP3A4.1, respectively. In addition, we found that the mechanism of inhibition was non-competitive inhibition in RLM and mixed inhibition in HLM. In pharmacokinetic experiments, it was observed that after gavage administration of 48 mg/kg napabucasin and 20 mg/kg arbidol, napabucasin inhibited the metabolism of arbidol *in vivo* and significantly changed the pharmacokinetic parameters of arbidol, such as AUC_(0-t) and AUC_(0-∞), in rats. We also found that napabucasin increased the AUC_(0-t) and AUC_(0-∞) of M6-1, the main metabolite of arbidol. This study provides a reference for the combined use of napabucasin and arbidol in clinical practice.

KEYWORDS

arbidol, napabucasin, drug–drug interactions, metabolism, CYP3A4

1 Introduction

In 1993, arbidol was introduced as a broad-spectrum antiviral drug to prevent and treat influenza infection (Boriskin et al., 2008). Arbidol 200 mg taken three times a day for about a week can reduce the duration of influenza by 1.7–2.65 days in clinical trials (Leneva et al., 2009). In recent years, coronavirus disease 2019 (COVID-19) has posed a significant threat to respiratory diseases and lung infections (Kirtipal et al., 2020; Vellingiri et al., 2020). Arbidol has been widely used for the prevention of COVID-19 and to improve the control of severe acute respiratory syndrome coronavirus 2 (SARS-CoV-2) infection (Nguyen et al., 2021; Zhou et al., 2021). Other applications of arbidol can be found as well. For example, studies showed that arbidol was also an effective and safe way to treat verruca plantaris and that topical administration of arbidol was more acceptable to patients (Chen et al., 2020).

COVID-19 symptoms are commonly treated with combinations of drugs, but they can also be harmful. For example, the combination of lopinavir/ritonavir (LPV/r) and arbidol will be a risk factor for liver injury in patients with non-critical COVID-19 (Cai et al., 2020). Studies reported that when LPV/r was combined with arbidol, the C_{max} of arbidol was increased and the $AUC_{(0-\infty)}$ of arbidol was significantly increased from 705.6 to 1250.3 ng/mL*h (Huang et al., 2021). In addition, pharmacokinetic and metabolic differences caused by administration of arbidol were found in male and female rats. When arbidol was used in combination with the famous Chinese medicine Lianhua Qingwen to treat COVID-19 (Liu et al., 2021), the levels of eosinophils and lymphocytes in patients were increased, which indicated that the combination was helpful in treating the progression of COVID-19.

In cancer treatment, napabucasin is a therapy that targets signal transducer and activator of transcription 3 (STAT3) pathways (Hubbard and Grothey, 2017; Chang et al., 2019). Several types of cancer can be treated with napabucasin alone or in combination, including advanced colorectal cancer, pancreatic cancer, and squamous cell carcinoma (Hubbard and Grothey, 2017). Furthermore, napabucasin administration in rats inhibits both apoptosis and oxidative stress, protecting neonatal rat neuronal cells from damage (Wang et al., 2019). There is a possibility that napabucasin could be used in the future to treat brain damage.

Drugs are often used in combination during the treatment of cancer, as cancer patients were also found to be affected with COVID-19 (Liu et al., 2020; Brito-Dellan et al., 2022). However, drug-drug interactions (DDI) between napabucasin and the antiviral drug arbidol have not been reported previously. Therefore, rapid detection of plasma levels of arbidol and its

metabolite was established by using ultra-performance liquid chromatography–tandem mass spectrometry (UPLC-MS/MS), and further studies of its interaction with napabucasin were conducted *in vitro* and *in vivo*.

2 Materials and methods

2.1 Chemicals and reagents

Arbidol and its metabolite, M6-1, were obtained from Shanghai Canspec Scientific Instruments Co., Ltd. (Shanghai, China). Lopinavir, used as the internal standard (IS), and napabucasin were also purchased from Shanghai Canspec Scientific Instruments Co., Ltd. (Shanghai, China). Analytical instruments were filled with acetonitrile and methanol that were purchased from Merck (Darmstadt, Germany). Human liver microsomes (HLMs) and CYP3A4.1 were obtained from iPhase Pharmaceutical Services Co., Ltd. (Beijing, China). Reduced nicotinamide adenine dinucleotide phosphate (NADPH) was obtained from Roche Pharmaceutical Ltd. (Basel, Switzerland). A Milli-Q Ultrapure Water System (Millipore, Bedford, United States) was used to produce purified water.

2.2 Instruments and UPLC-MS/MS

Quantitative analysis was performed using a combination of the Waters Xevo TQ-S triple quadrupole tandem mass spectrometer and a Waters ACQUITY UPLC I-Class system (Milford, MA, United States). The instrument was equipped with an automatic

TABLE 1 Analytical parameters of arbidol, M6-1, and internal standard (IS).

Analyte	Ionization mode	Parent (m/z)	Daughter (m/z)	Cone (V)	Collision (V)
Arbidol	ESI ⁺	478.80	433.80	20	16
M6-1	ESI ⁺	494.83	369.87	10	12
IS	ESI ⁺	629.61	182.98	10	15

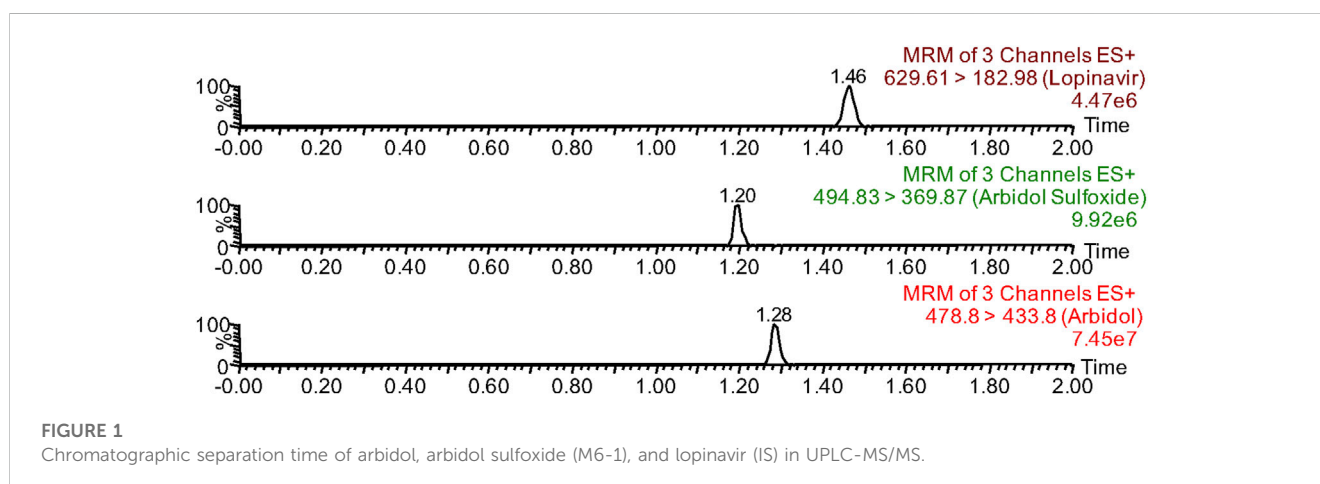


FIGURE 1

Chromatographic separation time of arbidol, arbidol sulfoxide (M6-1), and lopinavir (IS) in UPLC-MS/MS.

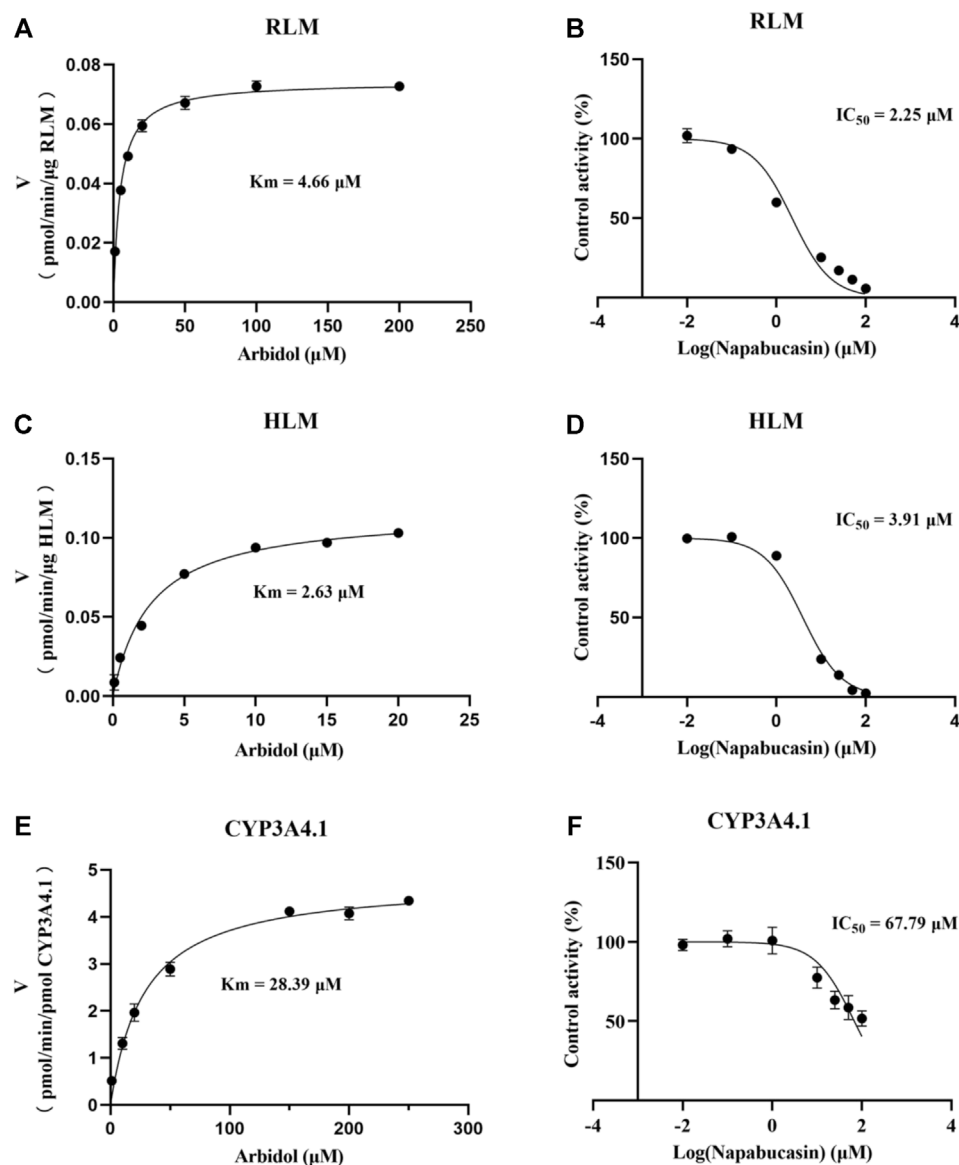


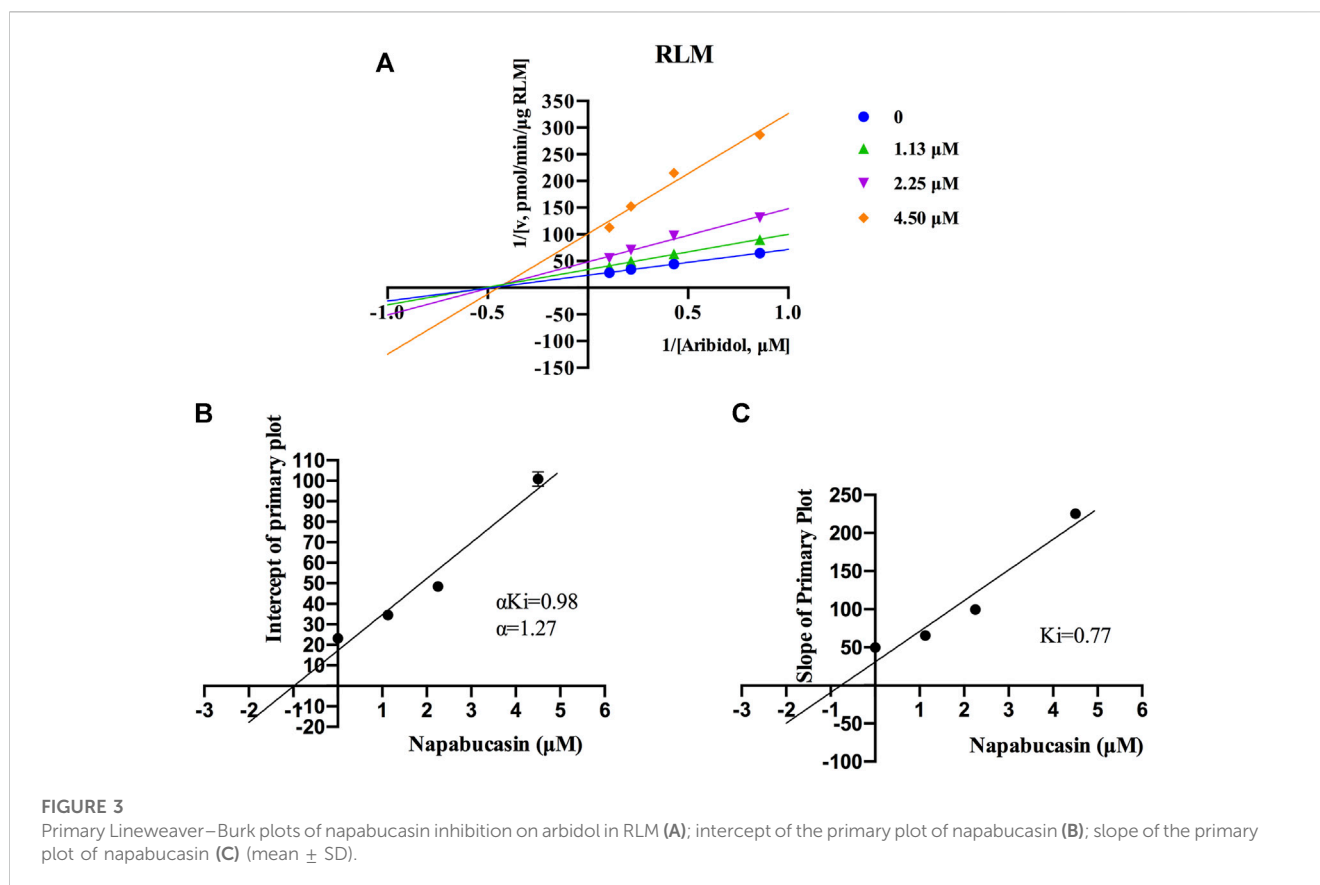
FIGURE 2

Michaelis constant of arbidol and half-maximal inhibitory concentration (IC_{50}) curve of napabucasin on arbidol in RLM (A, B), HLM (C, D), and CYP3A4.1 (E, F), respectively (mean \pm SD).

sample injection program to achieve fully automatic sample filling and accurate detection. The ACQUITY BEH C18 column (2.1 mm \times 50 mm, 1.7 μm ; Milford, MA, United States) used for accurate separation of the analytes in the sample at 40°C with acetonitrile (solvent A) and 0.1% formic acid (solvent B) as mobile phases. The gradient elution program was conducted at a flow rate of 0.4 mL/min as follows: 0–0.5 min (10% A+ 90% B), 0.5–1.0 min (10% A increase to 90% A), 1.0–1.4 min (maintain 90% A+ 10% B), 1.4–1.5 min (90% A decrease to 10% A), and 1.5–2.0 min (10% A+ 90% B). Triple quadrupole mass spectrometers were equipped with electrospray ionization (ESI) sources, and multiple reaction monitoring (MRM) modes were used for quantification. Depending on the ion, we selected different ion monitoring voltage conditions, and the results are shown in Table 1.

2.3 Preparation of rat liver microsomes (RLMs)

Rat livers were weighed and homogenized with cold 0.01 mM phosphate-buffered saline (PBS, pH 7.4) containing 0.25 mM sucrose. The homogenates were centrifuged at 11,000 rpm at 4°C for 15 min, and the supernatants were centrifuged repeatedly. Then, the supernatants were transferred to new tubes, centrifuged at 75,600 \times g for 2 h, the supernatants were discarded, and three or four times the volume of cold 0.01 mM phosphate-buffered saline was added to the precipitate for homogenization. Finally, the protein concentrations were determined using the Pierce™ BCA Protein Assay Kit (Thermo Scientific) (He et al., 2018).



2.4 *In vitro* DDI studies in RLM, HLM, and CYP3A4.1

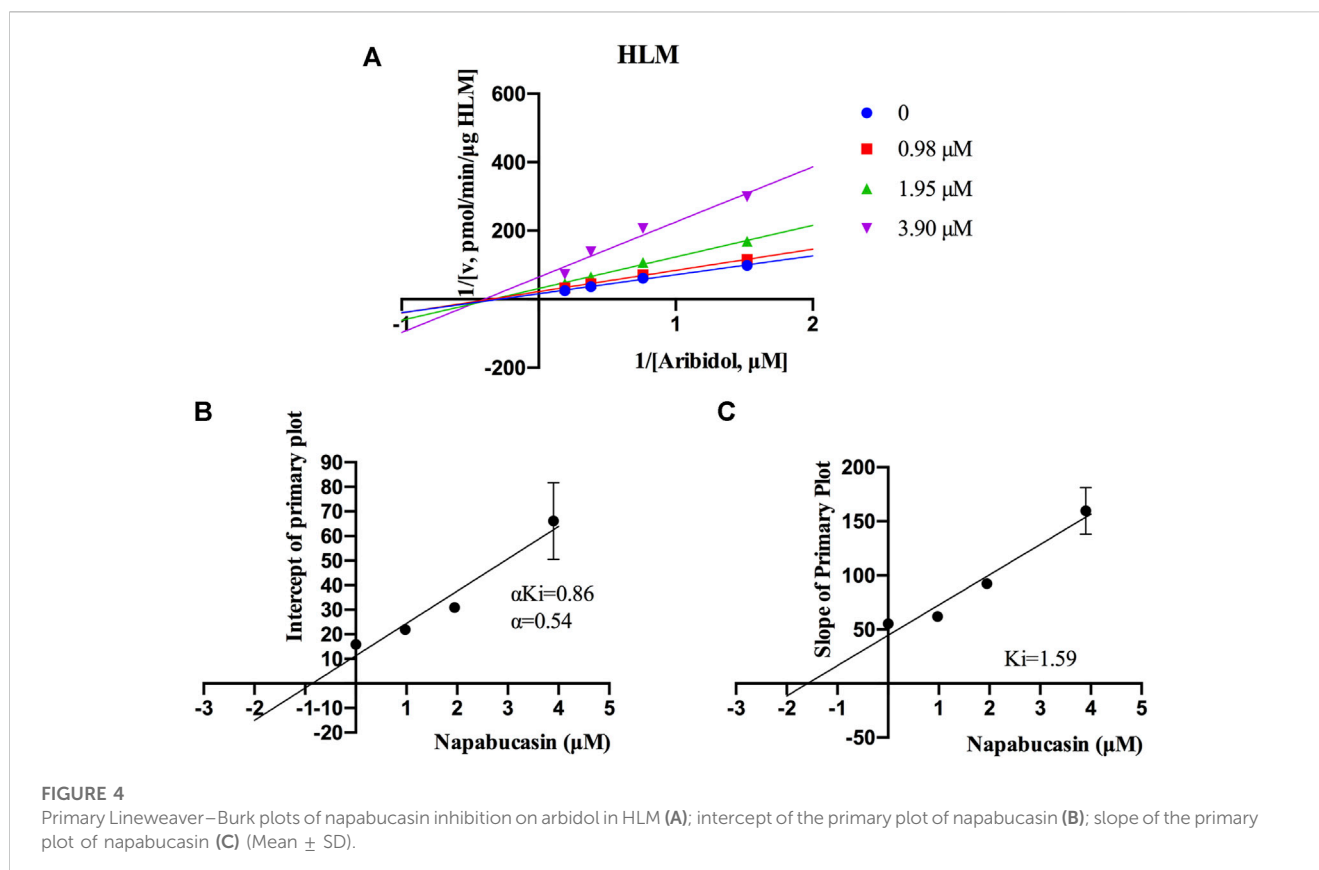
The 200 μL incubation system was as follows: 0.3 mg/mL RLM (0.3 mg/mL HLM), 1 mM NADPH, pH 7.4 phosphate buffer, and arbidol. Arbidol was used in a range of concentrations (1, 5, 10, 20, 50, 100, and 200 μM) to determine K_m (Michaelis constant) in RLM. In HLM, a series of concentrations (0.1, 0.5, 2, 5, 10, 15 and 20 μM) of arbidol were used to determine K_m . In CYP3A4.1, the following concentrations of arbidol were used to determine K_m : 1, 10, 20, 50, 150, 200, 250 μM . Napabucasin was established at concentrations 0.01, 0.1, 1, 10, 25, 50, and 100 μM to determine its IC_{50} (half-maximal inhibitory concentration) versus arbidol (4.66, 2.63, and 28.39 μM in RLM, HLM, and CYP3A4.1, respectively, according to their K_m values). In addition, the changes in Michaelis–Menten curves in the presence of napabucasin were investigated in RLM and HLM. To study the type of inhibition mechanism, we used the Lineweaver–Burk plot analysis and inhibition constant (K_i and αK_i) calculation, where drug concentrations were set as follows: 1.17, 2.33, 4.66, and 9.32 μM for arbidol and 0, 1.13, 2.25, and 4.50 μM for napabucasin in RLM. In HLM, the concentrations of arbidol were 0.66, 1.32, 2.63, and 5.26 μM , and those of napabucasin were 0, 0.98, 1.95, and 3.90 μM . The components in the incubation system were pre-incubated at 37°C for 5 min. After adding NADPH, the reaction was initiated and incubated at 37°C for 30 min. After the stop reaction

at -80°C , 400 μL of acetonitrile and 20 μL of IS (lopinavir 200 ng/mL) were added for post-treatment, vortexed for 2 min, and centrifuged at 13,000 rpm for 10 min. Finally, the supernatant was used for quantitative analysis using UPLC-MS/MS.

2.5 *In vivo* pharmacokinetic experiments

Sprague–Dawley rats (200 \pm 20 g, approximately 6 weeks) were supplied by The First Affiliated Hospital of Wenzhou Medical University and used for the pharmacokinetic experiments. Except for fasting 12 h before the start of pharmacokinetic experiments, rats were fed on a standard rodent diet and kept in a 12-h light–dark cycle environment at 20°C–26°C and 55 \pm 15% relative humidity.

Rats were randomly divided into two groups of five each. Arbidol and napabucasin were soluble in 0.5% carboxymethylcellulose sodium solution (CMC-Na). The treatment group was given 48 m/kg napabucasin by gavage, and the control group was given 0.5% CMC-Na solution of the same volume. Thirty minutes after the treatment, each rat was given a single administration of 20 mg/kg of arbidol. Blood samples were obtained from the caudal veins at different times (0.5, 0.75, 1, 1.5, 2, 4, 6, 8, 12, and 24 h). A volume of 10 μL of IS (200 ng/mL) and 300 μL of acetonitrile was added to 100 μL of plasma and mixed in the Eppendorf tube. The UPLC-MS/MS analysis of the supernatant was conducted after centrifuging the mixture at 13,000 rpm for 10 min.



2.6 Data analysis

Calculations of IC_{50} values and enzyme kinetic parameters were carried out using GraphPad Prism 6.0 (GraphPad software Inc., CA, United States). The key pharmacokinetic parameters were analyzed using DAS software (Version 3.0 software, Shanghai University of Traditional Chinese Medicine, China). Means \pm standard deviations (SD) were calculated for each experiment.

3 Results

3.1 Method validation

The methodologies were compliant with the standards of the EMA and FDA for bioanalytical methods (U.S. Department of Health and Human Services, Food and Drug Administration, FDA, and Center for Drug Evaluation and Research, CDER, 2018; European Medicines Agency, 2011). In this paper, a methodology was presented that enables the quantitative analysis of arbidol in plasma along with its main metabolite, M6-1. Arbidol, lopinavir, and M6-1 could be detected separately in UPLC-MS/MS without endogenous interference, and their retention times were 1.28, 1.46, and 1.20 min, respectively (Figure 1). The concentration ranges of arbidol and M6-1 for standard curves were 1–200 ng/mL and 1–100 ng/mL, respectively. Their correlation coefficients were $r^2 > 0.99$. Both arbidol and M6-1 had acceptable precision

and accuracy with a low limit of quantitation (LLOQ) of 1.0 ng/mL.

3.2 Effects of napabucasin on the metabolism of arbidol *in vitro*

Using the aforementioned incubation system, in RLM, the K_m of arbidol was 4.66 μ M, the IC_{50} of napabucasin for arbidol was 2.25 μ M, and the metabolic rate of arbidol was decreased to 3.73% in the presence of 100 μ M napabucasin. In HLM, the K_m of arbidol was 2.63 μ M and the IC_{50} of napabucasin for arbidol was 3.91 μ M (Figure 2). In addition, the Michaelis–Menten parameters for napabucasin inhibition of arbidol had remarkable changes (Supplementary Figures S1, S2), where V_{max} and CL_{int} were decreased to 43.1% and 18.2% in RLM and 59.0% and 50.0% in HLM, respectively. Among the types of inhibition mechanisms, arbidol inhibited by napabucasin in RLM was non-competitive inhibition because the Lineweaver–Burk plot showed that the family of straight lines intersected on the negative semi-axis of y, and the parameters K_i and αK_i ($\alpha = 1.27$) were 0.77 and 0.98 μ M, respectively (Figure 3). In HLM, the inhibition type of napabucasin on arbidol was mixed inhibition, as indicated by the Lineweaver–Burk plot, which showed that a family of straight lines intersected in the third quadrant, and the parameters K_i and αK_i ($\alpha = 0.54$) were 1.59 and 0.86 μ M, respectively (Figure 4). Moreover, in CYP3A4.1, the K_m and IC_{50} values of

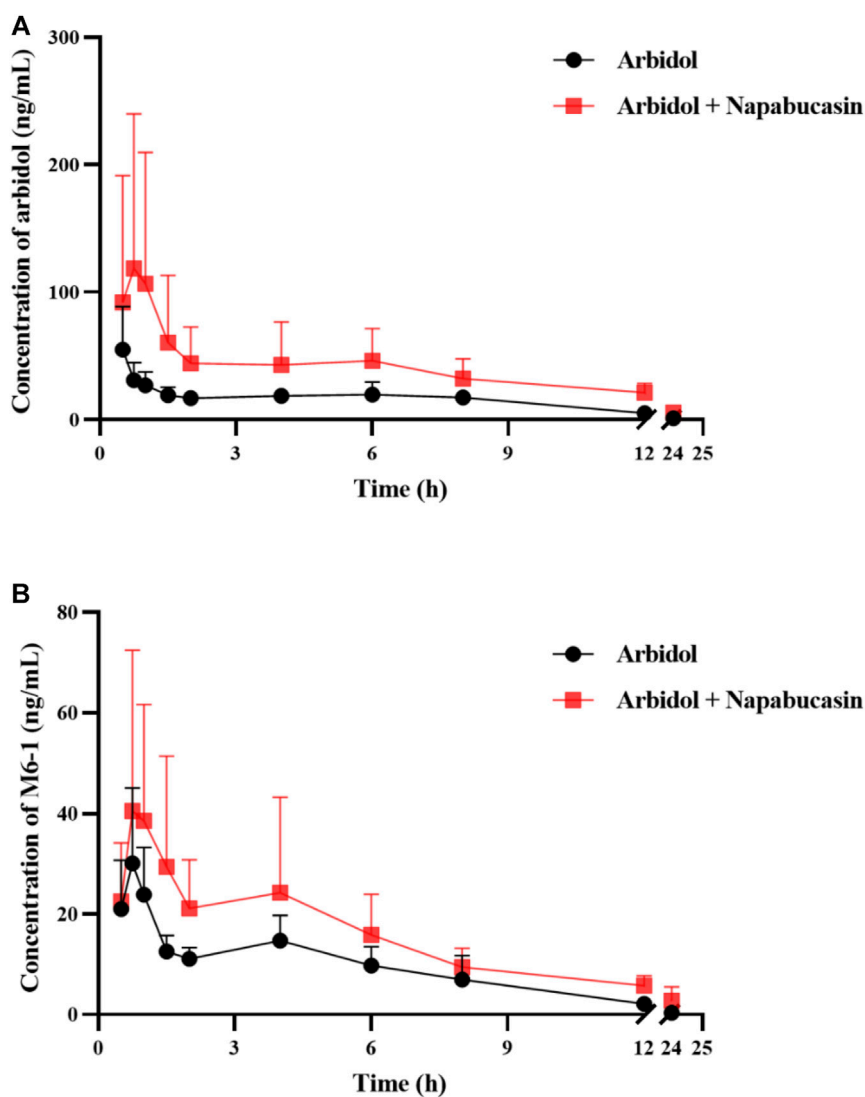


FIGURE 5 Average plasma concentration–time curve of arbidol (A) and its metabolite M6-1 (B) in the control group (arbidol alone) and the treatment group (arbidol with napabucasin) ($n = 5$).

TABLE 2 Main pharmacokinetic parameters of arbidol in the control group (arbidol alone) and the treatment group (arbidol with napabucasin) of rats ($n = 5$; mean \pm SD).

Parameter	Arbidol	Arbidol + napabucasin
AUC _(0-t) (ng/mL*h)	235.99 \pm 46.18	671.47 \pm 297.18*
AUC _(0-∞) (ng/mL*h)	277.60 \pm 15.00	719.51 \pm 276.83**
$t_{1/2\alpha}$ (h)	5.87 \pm 2.54	6.27 \pm 2.64
T_{max} (h)	0.60 \pm 0.14	1.05 \pm 0.57
CL _r /F (L/h/kg)	72.21 \pm 3.75	30.32 \pm 8.34***
C _{max} (ng/mL)	56.25 \pm 32.61	143.33 \pm 126.28

$p < 0.05$, $p < 0.01$, and $p < 0.001$, compared with the arbidol alone. AUC, area under the plasma concentration–time curve; $t_{1/2\alpha}$, elimination half time; T_{max} , peak time; CL_r/F, plasma clearance; and C_{max}, maximum plasma concentration.

TABLE 3 Main pharmacokinetic parameters of M6-1 in the control group (arbidol alone) and the treatment group (arbidol with napabucasin) of rats ($n = 5$; mean \pm SD).

Parameter	Arbidol	Arbidol + napabucasin
AUC _(0-t) (ng/mL*h)	139.67 \pm 31.87	248.96 \pm 81.16*
AUC _(0-∞) (ng/mL*h)	134.38 \pm 30.92	259.55 \pm 80.21*
t _{1/2z} (h)	3.77 \pm 1.23	5.12 \pm 1.94
T _{max} (h)	1.00 \pm 0.56	1.25 \pm 0.50
CL _z /F (L/h/kg)	156.64 \pm 42.82	82.87 \pm 24.17*
C _{max} (ng/mL)	31.08 \pm 13.11	48.52 \pm 28.46

$p < 0.05$, compared with the arbidol alone. AUC, area under the plasma concentration-time curve; t_{1/2z}, elimination half time; T_{max}, peak time; CL_z/F, plasma clearance; and C_{max}: maximum plasma concentration.

the assayed arbidol were 28.39 and 67.79 μ M, respectively (Figure 2). Due to its excessive size ($>10 \mu$ M), the mechanism of inhibition of napabucasin on arbidol in CYP3A4.1 was not explored further.

3.3 Effect of napabucasin on the metabolism of arbidol *in vivo*

The average plasma concentration-time curve of arbidol and its metabolite M6-1 in the control group (arbidol alone) and the treatment group (arbidol with napabucasin) is shown in Figure 5. The important pharmacokinetic parameters in rats are shown in Tables 2, 3. Compared to the control group, the AUC_(0-t) of arbidol in rats in the treatment group was increased by 1.85-fold, and the AUC_(0-∞) was increased by 1.59-fold. In addition, the parameters CL_z/F were reduced by 58.0% (Table 2), which indicated that the metabolism of arbidol was inhibited by napabucasin. We measured the levels of the main metabolite M6-1 in the plasma of rats and found that M6-1 levels in the treatment group were similarly affected compared to the control group. The AUC_(0-t) of M6-1 in rats from the treatment group was increased by 78.2%, and AUC_(0-∞) was increased by 93.1%. Interestingly, the parameters CL_z/F were reduced by 47.1% (Table 3). Based on the pharmacokinetic results, napabucasin inhibited arbidol metabolism in rats.

4 Discussion

Arbidol is a popular drug for the treatment of COVID-19, and its pharmacokinetic metabolism in the body is gradually attracting attention (Deng et al., 2013; Hu et al., 2021; Yu et al., 2022). In the context of the gradual implementation of individualized drug application, we established a rapid and effective detection method to detect the levels of arbidol and its metabolite using UPLC-MS/MS.

The chromatogram analysis results of UPLC-MS/MS showed that there was no interference between arbidol, M6-1, and IS during the detection process. When $1 < IC_{50} < 10 \mu$ M, it was considered medium inhibitory efficiency (Jin et al., 2015). The metabolic study of arbidol in the incubation system we established found that the IC₅₀ of napabucasin for arbidol was IC₅₀ = 2.25 μ M $< 10 \mu$ M in RLM and IC₅₀ = 3.91 μ M $< 10 \mu$ M in HLM. This indicated that napabucasin exhibited medium inhibition on the metabolism of arbidol in RLM and HLM. Additionally, napabucasin inhibited the

metabolism of arbidol to 3.73% in RLM. Among the many anti-tumor drugs, we also found that the metabolic inhibition rate of olmutinib, adagrasib, and sunitinib on arbidol was also below 10% (this part of the data has not yet been published). To prevent adverse reactions, it is recommended to pay attention to DDI when using chemotherapy drugs with arbidol to treat diseases in the clinic. Arbidol inhibition studies with napabucasin showed that there were differences between species *in vitro*. The type of inhibition mechanism was non-competitive inhibition in RLM, while the inhibition type was mixed inhibition in HLM. In addition, in HLM, Ki and αKi ($\alpha = 0.54$) were 1.59 and 0.86 μ M, respectively. However, the mechanism in CYP3A4.1 was not investigated due to its excessive IC₅₀.

Combination medications are used to treat critical patients with COVID-19 and cancer (Deng et al., 2020; Amani et al., 2021). Arbidol is mainly metabolized by the CYP3A4 isoenzyme in humans, so theoretically inducers or inhibitors of CYP3A4 will affect the metabolism of arbidol. LPV/r as protease inhibitors had a significant interaction with arbidol, which increased the C_{max} and AUC_(0-∞) of both drugs (Huang et al., 2021). In this experiment, napabucasin is found to be a bioactivator of quinone oxidoreductase 1 that generates reactive oxygen species (Chang et al., 2019; Froeling et al., 2019). Clinically, it is mainly used for the combination of gastric cancer and metastatic colon cancer in treating diseases (Li et al., 2015). Previous studies showed that *in vitro*, napabucasin is an inhibitor of the CYP2C9, CYP2C19, and CYP3A isozymes; *in vivo* DDI experimental clinical studies investigating the effect of napabucasin on the seven main cytochrome enzymes in the human body found that it may only cause moderate inhibition of CYP2B6 and has no induction or inhibitory effect on CYP1A2, 2C8, 2C9, 2C19, 2D6, 3A, or the BCRP/OAT3 (Dai et al., 2021). According to our results, the *in vivo* pharmacokinetic results of our study in rats are not consistent with this result, which showed that the combination of napabucasin and arbidol increased the concentration of arbidol in rats. Pharmacokinetic parameters were statistically significant, including AUC_(0-t) and AUC_(0-∞) (Table 2). Under the influence of napabucasin, the CL_z/F of both arbidol and its main metabolite M6-1 had been slowed compared to the drug alone. The slowdown of M6-1 metabolism may further affect the metabolism of arbidol *in vivo*, so future studies should pay attention to the plasma concentration of the metabolite.

The aforementioned results showed that napabucasin inhibited arbidol metabolism *in vivo* and *in vitro*. The differences in inhibitory

effects in RLM and HLM may come from differences between species, as the amount of CYP3A4 expressed was not the same between species. Previous studies reported that differences in sexes can be observed in arbidol metabolism, but unfortunately, this experiment did not compare the metabolic differences of napabucasin and arbidol between rat sexes. A future study in clinics should investigate the effect of napabucasin on arbidol metabolism in humans and whether gender affects the interaction between the two drugs.

5 Conclusion

The metabolism of arbidol in RLM and HLM was moderately inhibited by napabucasin *in vitro*, except for CYP3A4.1, with weak inhibition. Its inhibition mechanism was non-competitive in RLM and mixed inhibition (competitive and non-competitive) in HLM. Moreover, in rat pharmacokinetic studies, napabucasin inhibited the metabolism of arbidol and its main metabolite M6-1 in a subtle way. In future studies, more attention should be paid to the combination of these two drugs, and the DDI in humans needs to be further explored.

Data availability statement

The original contributions presented in the study are included in the article/[Supplementary Material](#); further inquiries can be directed to the corresponding author.

Ethics statement

The animal studies were approved by The First Affiliated Hospital of Wenzhou Medical University. The studies were conducted in accordance with the local legislation and institutional requirements. Written informed consent was obtained from the owners for the participation of their animals in this study.

References

- Amani, B., Amani, B., Zareei, S., and Zareei, M. (2021). Efficacy and safety of arbidol (umifenovir) in patients with COVID-19: a systematic review and meta-analysis. *Immun. Inflamm. Dis.* 9 (4), 1197–1208. doi:10.1002/iid3.502
- Boriskin, Y., Leneva, I., Pécheur, E., and Polyak, S. J. C. (2008). Arbidol: a broad-spectrum antiviral compound that blocks viral fusion. *viral fusion* 15 (10), 997–1005. doi:10.2174/092986708784049658
- Brito-Dellan, N., Tsoukalas, N., and Font, C. (2022). Thrombosis, cancer, and COVID-19. *Support Care Cancer* 30 (10), 8491–8500. doi:10.1007/s00520-022-07098-z
- Cai, Q., Huang, D., Yu, H., Zhu, Z., Xia, Z., Su, Y., et al. (2020). COVID-19: abnormal liver function tests. *J. Hepatol.* 73 (3), 566–574. doi:10.1016/j.jhep.2020.04.006
- Chang, A., Hsu, E., Patel, J., Li, Y., Zhang, M., Iguchi, H., et al. (2019). Evaluation of tumor cell-tumor microenvironment component interactions as potential predictors of patient response to napabucasin. *Mol. Cancer Res.* 17 (7), 1429–1434. doi:10.1158/1541-7786.MCR-18-1242
- Chen, L., Wu, Y., Gao, X., and Sun, Y. J. (2020). Topical arbidol for the treatment of verruca plantar: a case report. *Dermatol Ther.* 33 (6), e14497. doi:10.1111/dth.14497
- Dai, X., Karol, M., Hitron, M., Hard, M., Goulet, M., McLaughlin, C., et al. (2021). Napabucasin drug-drug interaction potential, safety, tolerability, and pharmacokinetics

Author contributions

JN: conceptualization, data curation, formal analysis, and writing—original draft. HX: writing—original draft, investigation, and methodology. Y-NL: writing—original draft and visualization. YY: writing—original draft, conceptualization, data curation, formal analysis, and writing—review and editing. R-AX: writing—review and editing, project administration, resources, software, supervision, and validation.

Funding

The author(s) declare that no financial support was received for the research, authorship, and/or publication of this article.

Conflict of interest

The authors declare that the research was conducted in the absence of any commercial or financial relationships that could be construed as a potential conflict of interest.

Publisher's note

All claims expressed in this article are solely those of the authors and do not necessarily represent those of their affiliated organizations, or those of the publisher, the editors, and the reviewers. Any product that may be evaluated in this article, or claim that may be made by its manufacturer, is not guaranteed or endorsed by the publisher.

Supplementary material

The Supplementary Material for this article can be found online at: <https://www.frontiersin.org/articles/10.3389/fphar.2023.1292354/full#supplementary-material>

following oral dosing in healthy adult volunteers. *Orig. Manuscr.* 10 (8), 824–839. doi:10.1002/cpdd.961

Deng, L., Li, C., Zeng, Q., Liu, X., Li, X., Zhang, H., et al. (2020). Arbidol combined with LPV/r versus LPV/r alone against Corona Virus Disease 2019: a retrospective cohort study. *Virus Dis. 2019 A Retrospect. cohort study* 81 (1), e1–e5. doi:10.1016/j.jinf.2020.03.002

Deng, P., Zhong, D., Yu, K., Zhang, Y., Wang, T., and Chen, X. (2013). Pharmacokinetics, metabolism, and excretion of the antiviral drug arbidol in humans. *Antimicrob. Agents Chemother.* 57 (4), 1743–1755. doi:10.1128/AAC.02282-12

European Medicines Agency (2011). *Guideline on bioanalytical method validation, committee for medicinal products for human use (CHMP)* (Accessed February 1, 2021). Available at: <https://www.ema.europa.eu/en/bioanalytical-method-validation>.

Froeling, F., Swamynathan, M., Deschênes, A., Chio, I., Brosnan, E., Yao, M., et al. (2019). Bioactivation of napabucasin triggers reactive oxygen species-mediated cancer cell death. *Clin. Cancer Res.* 25 (23), 7162–7174. doi:10.1158/1078-0432.CCR-19-0302

He, J., Fang, P., Zheng, X., Wang, C., Liu, T., Zhang, B., et al. (2018). Inhibitory effect of celecoxib on agomelatine metabolism *in vitro* and *in vivo*. *Drug Des. Devel Ther.* 12, 513–519. doi:10.2147/DDDT.S160316

- Hu, Y., Zuo, M., Wang, X., Wang, R., Li, L., Lu, X., et al. (2021). Pharmacokinetic interactions between the potential COVID-19 treatment drugs lopinavir/ritonavir and arbidol in rats. *J. Zhejiang Univ. Sci. B* 22 (7), 599–602. doi:10.1631/jzus.B2000728
- Huang, X., Li, C., Li, C., Li, Z., Li, X., Liao, J., et al. (2021). CYP2C19 genotyping may provide a better treatment strategy when administering escitalopram in Chinese population. *Front. Pharmacol.* 12, 730461. doi:10.3389/fphar.2021.730461
- Hubbard, J., and Grothey, A. J. D. (2017). Napabucasin: an update on the first-in-class cancer stemness inhibitor. *Drugs* 77 (10), 1091–1103. doi:10.1007/s40265-017-0759-4
- Jin, C., He, X., Zhang, F., He, L., Chen, J., Wang, L., et al. (2015). Inhibitory mechanisms of celastrol on human liver cytochrome P450 1A2, 2C19, 2D6, 2E1 and 3A4. *Xenobiotica* 45 (7), 571–577. doi:10.3109/00498254.2014.1003113
- Kirtipal, N., Bharadwaj, S., and Kang, S. J. I. (2020). From SARS to SARS-CoV-2, insights on structure, pathogenicity and immunity aspects of pandemic human coronaviruses. *Review* 85, 104502. doi:10.1016/j.meegid.2020.104502
- Leneva, I., Russell, R., Boriskin, Y., and Hay, A. J. (2009). Characteristics of arbidol-resistant mutants of influenza virus: implications for the mechanism of anti-influenza action of arbidol. *Antivir. Res.* 81 (2), 132–140. doi:10.1016/j.antiviral.2008.10.009
- Li, Y., Rogoff, H., Keates, S., Gao, Y., Murikipudi, S., Mikule, K., et al. (2015). Suppression of cancer relapse and metastasis by inhibiting cancer stemness. *Res. ARTICLE* 112 (6), 1839–1844. doi:10.1073/pnas.1424171112
- Liu, C., Zhao, Y., Okwan-Duodu, D., Basho, R., and Cui, X. (2020). COVID-19 in cancer patients: risk, clinical features, and management. *Cancer Biol. Med.* 17 (3), 519–527. doi:10.20892/j.issn.2095-3941.2020.0289
- Liu, L., Shi, F., Tu, P., Chen, C., Zhang, M., Li, X., et al. (2021). Arbidol combined with the Chinese medicine Lianhuaqingwen capsule versus arbidol alone in the treatment of COVID-19. *Med. Baltim.* 100 (4), e24475. doi:10.1097/MD.00000000000024475
- Nguyen, H., Salkeld, J., Agarwal, S., and Goodman, A. (2021). Compassionate use of REGN-COV2 in the treatment of COVID-19 in a patient with impaired humoral immunity. *Clin. Infect. Pract.* 12, 100089. doi:10.1016/j.clinpr.2021.100089
- U.S. Department of Health and Human Services Food and Drug Administration (FDA), Center for Drug Evaluation and Research (CDER) (2018). Center for veterinary medicine (CVM), bioanalytical method validation guidance for industry. *Cent. Drug Eval. Res.* Available at: <https://www.fda.gov/regulatory-information/search-fda-guidance-documents/bioanalytical-method-validation-guidance-industry>
- Vellingiri, B., Jayaramayya, K., Iyer, M., Narayanasamy, A., Govindasamy, V., Giridharan, B., et al. (2020). COVID-19: a promising cure for the global panic. *Sci. Total Environ.* 725, 138277. doi:10.1016/j.scitotenv.2020.138277
- Wang, J., Feng, H., Li, Z., and Zhang, X. (2019). Napabucasin prevents brain injury in neuronal neonatal rat cells through suppression of apoptosis and inflammation. *Microb. Pathog.* 128, 337–341. doi:10.1016/j.micpath.2019.01.019
- Yu, M., Wang, D.-C., Li, S., Lei, Y.-H., Wei, J., and Huang, L.-Y. (2022). Meta-analysis of arbidol versus lopinavir/ritonavir in the treatment of coronavirus disease 2019. *J. Med. Virol.* 94 (4), 1513–1522. doi:10.1002/jmv.27481
- Zhou, X., Hou, H., Yang, L., Ding, G., Wei, T., Li, C., et al. (2021). Arbidol is associated with increased in-hospital mortality among 109 patients with severe COVID-19: a multicenter, retrospective study. *J. Glob. Health* 11, 05017. doi:10.7189/jogh.11.05017